Biochemical and Biophysical Research Communications **280,** 312–318 (2001)
doi:10.1006/bbrc.2000.4115, available online at http://www.idealibrary.com on IDEAL®

Microenvironment of Endosomal Aqueous Phase Investigated by the Mobility of Microparticles Using Fluorescence Correlation Spectroscopy

Naoto Yoshida,[1] Masataka Kinjo, and Mamoru Tamura
Laboratory of Supramolecular Biophysics, Research Institute for Electronic Science, Hokkaido University, N12W6, Kita-ku, Sapporo 060-0812, Japan

Received December 2, 2000

Temporal observation of the dynamic behavior of molecules in cells gives information about the physiological environment at the region of interest. Here we report the direct measurement of the mobility of rhodamine-labeled microparticles (14 and 35 nm in diameter) ingested in endosomes of cultured bovine aortic endothelial cells using fluorescence correlation spectroscopy (FCS). The fluctuation of fluorescent signals from microparticles were measured by FCS. Obtained autocorrelation functions (FAFs) were analyzed by the 2-D multicomponent model according to an evaluation procedure we newly developed. It was found that microparticles moved freely in endosomes with average diffusion coefficients of 4.3×10^{-8} and 2.7×10^{-8} cm^2 s^{-1} for 14 and 35 nm, which were 45% slower than in water. This result implies that the endosomal aqueous phase is homogeneous with the viscosity about 2.2 times of water. Our study also proposes the new use of FCS for investigation of the internal space of organelles.

Key Words: **fluorescence correlation spectroscopy; endocytosis; single cell measurement.**

Fluorescence correlation spectroscopy (FCS) is an unique method (1–6) to determine the diffusional properties of fluorescent molecules based on the measurement of fluorescence autocorrelation function (FAF) originated from fluorescence intensity fluctuations in a defined very small observation volume of subfemtoliter. In recent years, FCS combined with a confocal optical system has been applied to investigate various biophysical and biochemical processes *in vitro* (7–11). Moreover, the subjects have spread to direct single living cell measurement of various intracellular phenomena, including the diffusional characteristics of microparticles injected into cytoplasmic space (12) and identification of green fluorescence protein (GFP) fusion proteins in different areas in a single cell (13). In addition, a recent study reported on the protein movement in squid giant axons (14). These reports emphasize not only the utility of FCS as a sensitive determination tool for fluorescent molecules in single-cell measurement but also the importance of *in vivo* study for systematic and hierarchical understanding of the dynamic structure of individual cell activity.

We are applying FCS to the investigation of the physiological microenvironment of organelles in living cells (Fig. 1). Various organelles have their own specific functions in which macromolecules, such as enzyme, are produced, digested and/or transported. The microenvironment of their internal space is the main determinant of the dynamics of macromolecules. However, due to very tiny volume of organelles, other methodological approaches used for the study on the mobility of molecules in cytoplasm such as fluorescence recovery after photobleaching (FRAP) (15–18) cannot give detailed information about them.

Endosome is a kind of organelle distributed in eukaryotic cells having the functions in which macromolecules (e.g., low density proteins and transferrin) ingested by endocytosis are sorted and delivered (19–26). The physiological properties of endosomal internal space are supposed to change continuously during the endocytosis process from the early endosome to the late endosome. However, the details are still unknown due to the lack of method, except for the finding that pH decreases from 6.2 to 4.5 with the processing (27).

In this study, using FCS, we directly measured the dynamic features of rhodamine-labeled latex microparticles 14 and 35 nm in diameter in endosomal aqueous phase of cultured bovine aortic endothelial cells ingested by naturally occurred fluid-phase endocytosis. The question is whether the microparticles move freely in endosomes, the answer to which will also provide

[1] To whom correspondence should be addressed. Fax: +81-11-706-4964. E-mail: nyoshida@imd.es.hokudai.ac.jp.

0006-291X/01 $35.00

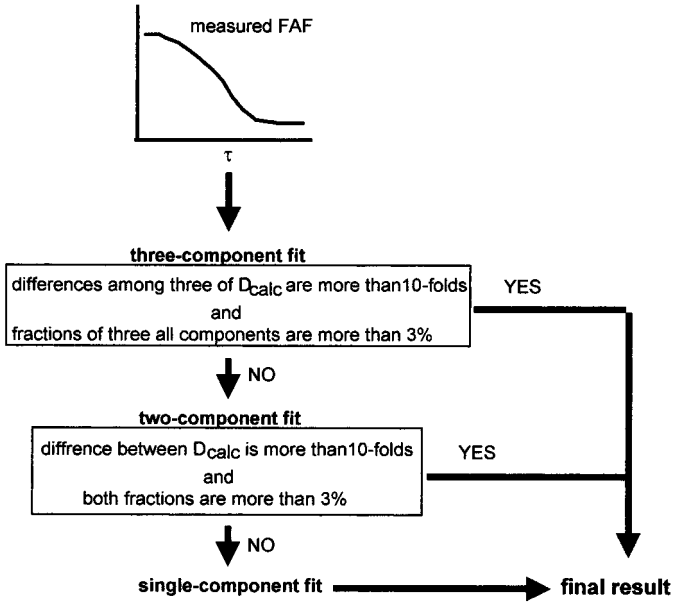

FIG. 1. Flow chart of evaluation procedure for FCS cell measurement.

information about microenvironment of the aqueous phase.

Previous to the cell measurement, we measured FAFs of the microparticles dispersed in water with changing the viscosity and pH. Obtained diffusion coefficients compared them with theoretical ones. Based on the results, the accuracy of FCS measurement and the characteristics of the microparticles are discussed.

Then FAFs of the microparticles in endosomes were measured at various points in cells. According to an evaluation procedure that we first developed, multicomponent fitting of each FAF gave two or three components having different diffusion coefficients. Based on statistical analysis of these components, the distinction between components that originated from the motion of microparticles in the endosomal space and those with other origins are discussed. Comparing the mobility of the microparticles in endosomes with that in aqueous solutions and cytoplasm, the microenvironment of the endosomal aqueous phase were evaluated.

MATERIALS AND METHODS

Microparticles. Carboxylate-modified and rhodamine-labeled latex microparticles (Fluospheres, 14 and 35 nm in diameter; Molecular Probes, Eugene, OR) were dispersed in purified water or culture medium and sonicated for 30 minutes before FCS measurements in order to avoid the aggregation.

Cell culture. Bovine aortic endothelial cells (purchased from Dainihon Seiyaku, Osaka, Japan) were grown in 5% CO_2–95% air at 37°C in Dulbecco's modified Eagle medium (DMEM) supplemented with 9% fetal bovine serum and 1% (v/v) aqueous solution of antibiotics (containing 10,000 units/ml penicillin, 10,000 μg/ml streptomycin, 25 μg/ml amphotericin B and 0.85% sodium chloride) on the chambered cover glass. Cells were used for measurement at >70% confluence.

FCS setup. Our FCS system (ConfoCor, Carl Zeiss Jena GmbH, Jena, Germany) consisted of, around an inverted microscope equipped with a water immersion objective lens (C-Apochromat, 40×, 1.2 NA; Carl Zeiss), a CW Ar^+ laser, an avalanche photodiode (SPCM-200-PQ, EG&G, Quebec, Canada), and a digital correlator (ALV 5000/E, ALV GmbH, Langen, Germany). A pinhole 30 nm in diameter was set at in front of the photodiode. All samples were measured on Lab-Tek chambered cover glasses (Nalge Nunc International, Naperville, IL) with 140-μm-thick cover glasses on the bottom. Samples were excited by a 515-nm line of the laser (about 4 kW/cm^2) and the fluorescence from the detection volume (0.24 fl), separated by a dichroic mirror (>510 nm) and an emission filter (530–610 nm), was detected.

Measurement of microparticle diffusion in water. Microparticles were dispersed in purified water at the concentration of 2×10^{-3}% solid (w/w). The viscosity of water was changed by addition of sucrose from 0 to 40% (w/w) by 10% steps. Sample solution (0.3 ml) was placed on the chambered cover glass. Then, the confocal focus was fixed at 200 μm over the cover glass. For each sample, FAF measurement for 30 s was repeated five times at 10-s intervals at room temperature. Diffusion coefficients were calculated from measured FAFs by single-component fitting according to the 3-D model Equation [5] as follows:

$$g(\tau) = 1 + \frac{1}{N}\left(1 + \frac{\tau}{\tau_D}\right)^{-1}\left(1 + \frac{\tau}{s^2\tau_D}\right)^{1/2}. \quad [1]$$

In this equation, s is the experimental parameter defined as $\omega_z/2\omega_o$ where ω_o and ω_z are the radius and the z-axis length of the confocal volume, respectively. τ_D is the correlation time. s depends on the optical alignment, changing from five to seven. Therefore, before the sample measurements, FAFs of rhodamine 6G (R6G) aqueous solution were measured for 60 s five times at 10-s intervals, then authentic value of s and τ_D for R6G were obtained. τ_D is inversely proportional to the diffusion coefficient D. Diffusion coefficients of the samples were calculated from the ratio with the diffusion coefficient of R6G (2.8×10^{-6} cm^2 s^{-1}) (6) based on the following equation:

$$D = 2.8 \times 10^{-6} \times \tau_D(\text{R6G})/\tau_D(\text{sample})(\text{cm}^2\,\text{s}^{-1}). \quad [2]$$

Cell measurement. Microparticles were added to the culture medium at the concentration of $4 \times 10^{-5\%}$ solid (w/w). Thirty minutes after, cells were washed with phenol red-free Iscove's modified Dulbecco's medium (IMDM) several times to remove microparticles remaining in extracellular space and measurements were carried out. First, the target cell was visually selected and then the measuring point was determined in cytosolic space excluding the nucleus. Next, the emission intensity profile along the optical axis from a point close to the cover glass was recorded. The focal point (measurement field) was fixed at the point where maximum fluorescence intensity was observed. FAF was measured for 30 s. Numbers of measurement points were 23 from five cells and 17 from seven cells for 14- and 35-nm microparticles, respectively. The thickness of the cell was comparable to the z-axis length of the confocal volume (26). Thus, the 2-D model Equation [5] described below was used to fit measured FAFs,

$$g(\tau) = 1 + \frac{1}{N}\sum_i \frac{f_i}{1 + \frac{4D_i\tau}{\omega_o^2}}. \quad [3]$$

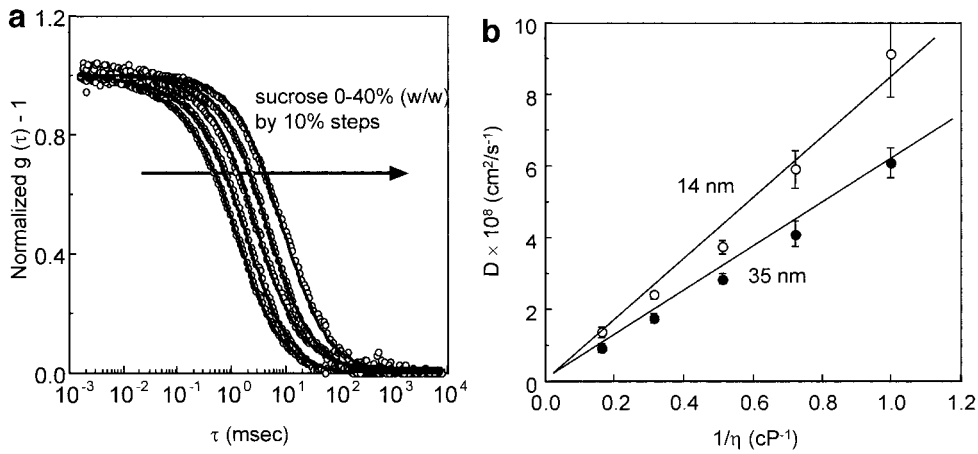

FIG. 2. (a) Normalized FAFs of microparticles 14 nm in diameter in water with various viscosities regulated by sucrose concentrations of 0–40% (w/w) by 10% steps, corresponding to viscosities of 1.0, 1.4, 2.0, 3.2, and 6.2 centipoise, respectively. (b) Plots of obtained diffusion coefficients vs inverse of viscosity for 14 nm (open circles) and 35 nm (closed circles). Each point is the average from four or five individual measurements. Error bars are the mean ± SEM.

Different from the 3-D model, the 2-D model directly provides the diffusion coefficient D. In this equation, f_i and D_i are the fraction and diffusion coefficient of component i, respectively. The radius of the confocal volume ω_0 was previously determined to be 224 nm by R6G measurement according to the equation below, with D of R6G:

$$\tau_D = \frac{\omega_0^2}{4D}. \quad [4]$$

Analysis for each FAF was carried out according to the procedure described as follows (a flow chart is also shown in Fig. 1).

First, three-component fitting was carried out. If the difference among two or three calculated diffusion coefficients was within 10-fold or one or two fractions comprised less than 3%, then the fit was redone using the two-component model. Then, if the difference between the two components was still within 10-fold or one of the two fractions accounted for less than 3%, finally, single-component fitting was redone.

RESULTS AND DISCUSSION

Microparticle diffusion in water. FAFs of 14-nm microparticles dispersed in water shifted to the right (Fig. 2a) with increases in the viscosity. This reflected the decrease of the diffusion coefficient of the microparticles. Analyzing these FAFs by a single-component fit based on Eqs. [1] and [2], which are shown by solid lines in Fig. 2a, the linear relationship between the diffusion coefficient and the inverse of viscosity is confirmed for each size of microparticle (Fig. 2b). This result agreed with the well-known Stokes–Einstein equation which describes the relationship, as for Brownian motion, between the diffusion coefficient of spherical objects and physical parameters of a homogeneous solvent, as

$$D = \frac{kT}{6\pi r\eta}, \quad [5]$$

where T is the absolute temperature, r is the radius of the sphere, η is the viscosity of the solvent, and k is the Boltzman constant. The averages of obtained diffusion coefficients of the microparticles in pure water without sucrose (1.0 cP) were 9.0×10^{-8} and 6.1×10^{-8} cm^2 s^{-1} for 14 and 35 nm, respectively. These values were 71 and 53% lower than those theoretically expected according to Eq. [5], 3.1×10^{-7} and 1.3×10^{-7} cm^2 s^{-1}. The ratio of the diffusion coefficient was 1.5 which was rather smaller than those theoretically expected from 2.5 of the size ratio of each microparticle. Two main reasons might account for these results: (i) small aggregation of microparticles might have been present even after 30 min sonication. (ii) The microparticles might not have been completely spherical, so that obtained diffusion coefficient could not agree well with Eq. [5]. Even if these phenomena actually occurred, the accuracy of FCS measurement was proved because the relationship between the diffusion coefficient and viscosity was accurately demonstrated. In addition, FAFs with the change in pH from 4 to 9 were measured and no significant difference among them was observed (data not shown). This suggested that the microparticles did not aggregate further and their physical properties were unchanged in endosomes and culture medium in this pH range.

FCS cell measurements. To clarify that the microparticles were actually ingested in endosomes under the culture conditions described under Materials and Methods, a fluorescence micrograph of cells was taken (Fig. 3a). This showed numerous endosomes with a variety of sizes and shapes with microparticles in the internal space distributed in the whole area of cytoplasm except in nucleoplasm. The incubation conditions for the micrograph were different from those for

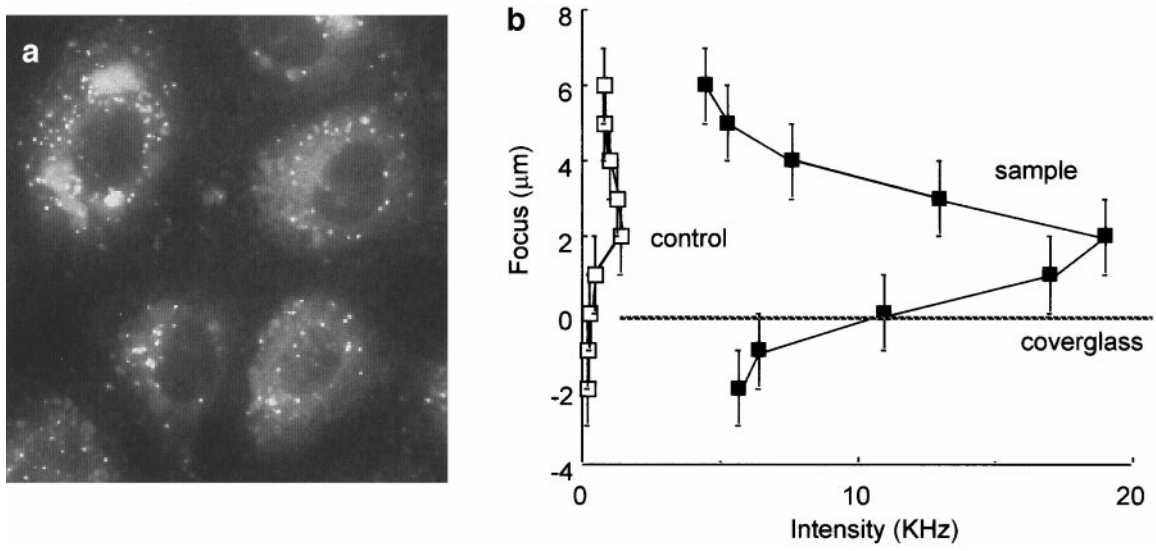

FIG. 3. (a) Emission micrograph of endothelial cells that ingested 14-nm microparticles in endosomes. (b) Emission intensity profile along the optical axis from a little under the cover glass through the cells recorded by focusing at 1-μm steps.

FCS measurements. To obtain high contrast, microparticles were added to the medium with a 50-fold higher concentration than that for FCS and incubation was carried out for 1 h. Then, for more confirmation, the profile of emission intensities was measured along the optical axis from the cover glass through the cytoplasmic space under the same conditions as for FCS measurements (Fig. 3b). Strong emissions were observed from the cells that contained microparticles in endosomes with the maximum intensity peak (up to 30 kHz) at around 2–3 μm over the cover glass and a half-maximum of 3–5 μm. In contrast, only very weak emissions (up to 3 kHz) were observed from the control cells without microparticles. These weak emissions from the control cells were mainly of intrinsic fluorescent molecules such as flavins (28), and were weak enough to be ignored compared to those of the microparticles. Considering that the thickness of cultured bovine aortic endothelial cells has been reported to be 4–8 μm (26), it was concluded that these strong emissions originated from microparticles in endosomes.

An example of the FAF of 14-nm microparticles in a cell is shown in Fig. 4a. Compared to that in water, the correlation curve shifted to the right, which means that there existed at least one component having a slower diffusion coefficient than that in water. Right-shifted curves were also observed for all measurements. In most measurements, FAFs could be analyzed by two- or three-component fitting according to Eq. [3] and the procedure described in Materials and Methods. The rest could be analyzed by a single-component fit. For all measurements, which were carried out from 10 to 70 min after the end of incubation, the major component with a fraction of >50% had a diffusion coefficient similar to that in water as shown in Figs. 4b and 4c. In

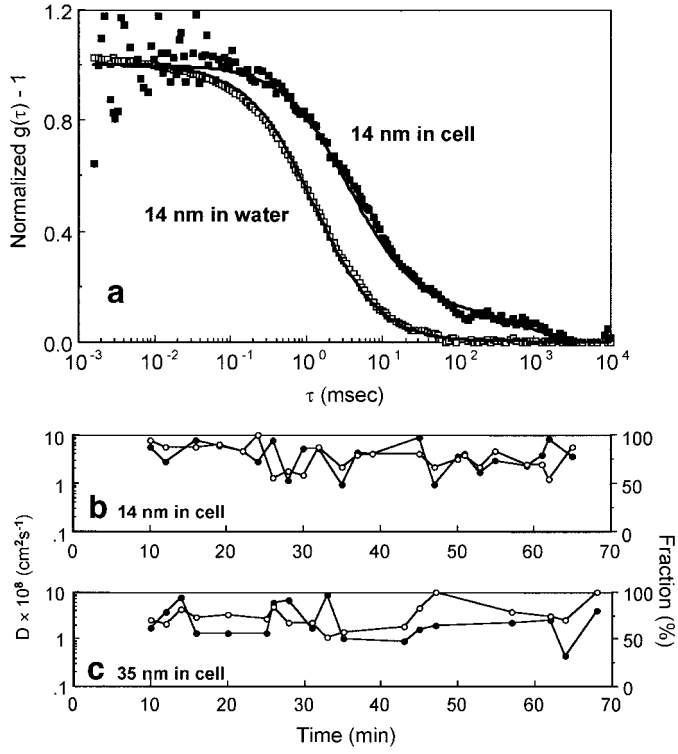

FIG. 4. (a) An example of FAF of 14-nm microparticles in endosomes (closed squares). By two-component fitting according to Eq. [5], a component having a faster diffusion coefficient of 3.6×10^{-8} $cm^2\ s^{-1}$ (87%) and another having a slower diffusion coefficient of 3.2×10^{-10} $cm^2\ s^{-1}$ (13%) were obtained. For comparison, FAF of same-sized microparticles in water is also shown (open squares). (b, c) Time course of obtained diffusion coefficient (closed circles) with the largest fraction (open circles) for all measurements of 14- and 35-nm microparticles. Abscissa indicates the time after the incubation of microparticles.

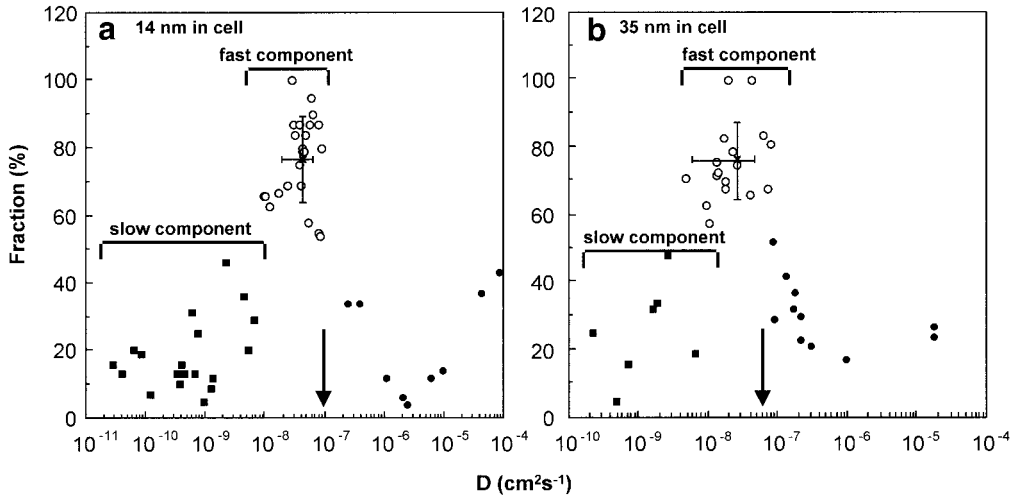

FIG. 5. Plots of all obtained diffusion coefficients vs their fractions from FAFs of 14-nm (a) and 35-nm (b) microparticles in cells. Number of points is more than that of measurement numbers since each datum was analyzed by multicomponent fitting. Crosses indicate the average of diffusions coefficient of the fast component. Error bars are the mean ± SEM. Arrows indicate the diffusion coefficients of microparticles in pure water obtained in this study.

addition, components having faster and/or slower diffusion was also observed in most measurements.

In some cases, weak photobleaching was observed during the measurement. The photobleaching might have been caused by two phenomena: (i) a small fraction of microparticles might have been fixed to inner surface of membrane of endosomes, and (ii) microparticles might have been trapped in small endosomes that completely overlapped the confocal volume. In both cases, fluorescence intensity could be decreased by photobleaching. Photobleaching could affect the measured FAF, but could not be the origin of the obtained slow diffusion since the photobleaching rate was much slower.

Obtained diffusion coefficients and their fractions were plotted for the evaluation (Figs. 5a and 5b). They were categorized into two groups; fast diffusion (10^{-8}–10^{-7} cm^2 s^{-1} with a fraction of more than 50%; open circles), slow diffusion ($<10^{-8}$ cm^2 s^{-1} with a fraction of less than 50%; closed squares). The rest, very fast diffusion ($>10^{-7}$ cm^2 s^{-1} closed circles), were excluded from the evaluation in this study since such the fast movement of the microparticles could not be considered in the cells as well in aqueous solutions.

Characterization of obtained components at the cell measurements. FCS is based on the measurement of fluorescence intensity fluctuation. In the cell measurements, the fluctuation was mainly due to continuous changes in the number of microparticles existing in the confocal volume. The changes presumably originated from two main factors: (i) movement of the microparticles in endosomal space, and (ii) movement and/or morphological changes of endosomes in cytoplasm. For the observation of the former [factor (i)] by FCS, frequent crossing of the microparticles through the boundary of the confocal volume must occur. Although the emission micrograph (Fig. 3a) suggested that numerous endosomes with various sizes and shapes existed in the cytoplasm, the size distribution of endosomes was not clarified due to its low spatial resolution. However there is some reports on the size and morphology of endosomes. It was reported (29) that the diameter of individual middle endosomes in brain astroglial cells was 500–1000 nm. Moreover, endothelial cells were reported to be able to ingest microparticles up to 800 nm in diameter (30). Therefore, there could be a sufficient number of endosomes which were large enough for the microparticles to diffuse and pass through the boundary of the confocal volume. Since there was Gauss distribution of excitation intensity in the confocal volume, the movement of microparticles and endosomes within it might have affected the FAF. However, this was negligible.

The components having fast diffusion coefficients (open circles in Figs. 5a and 5b) were attributed to the diffusion of the microparticles in the endosomal aqueous phase, mainly of the middle and late endosomes. The averages of obtained diffusion coefficients were 4.3×10^{-8} and 2.7×10^{-8} cm^2 s^{-1} for 14 and 35 nm, respectively, corresponding to approximately 45% of those in water.

The origin of slow diffusion (closed squares in Figs. 5a and 5b) seems to be, a part, the motion of endosomes in cytoplasmic space. It is known (26) that the motion of endosome is mediated by an intact cytoskeleton composed of microtubules, microfilaments, and intermediate filaments. And a recent study (29) reported that a large fraction of endosomes in rat brain astroglial cells moved very slowly (<0.04 μm/s) which is consistent with our result. The size of the early endosomes were

supposedly smaller those of the middle and late endosomes (31). Therefore the fluorescence intensity fluctuation from the early endosomes could make the slow diffusion reflected the motion of the endosomes themselves.

Microenvironment of endosomal aqueous phase. In a previous study (12) using FCS, it was reported that movement of microparticles of the same size injected in cytoplasm slowed down and are immobilized a few hours after injection, possibly due to binding to intracellular cytoskeleton. However, such phenomena were not observed in this study during the measurements up to about 1 h after the ingestion of microparticles in endosomes as demonstrated in Figs. 4b and 4c. Then, the results shown in Fig. 5 suggest that the average viscosity of endosomal internal phase is only about 2.2-fold of that of water, corresponding to 20% sucrose aqueous solution. These facts prove that the endosomal internal space is different from cytoplasm and almost homogeneous without microstructures and matrices such as microtubules and cytoskeletal compounds, etc., to which microparticles could bind.

The deviations of obtained diffusion coefficients might, in part, have been due to the difference of viscous properties of individual endosomes. In the early endosome, viscosity is expected to be almost same as that of water since its endosomal space is constructed by the ingestion of culture medium in which the viscosity is almost the same as water. In contrast, the late endosome is presumed to be slightly more viscous, because of fusion with the hydrolase-rich lysosome. Therefore, the variety of obtained value is consider to have reflected the viscosity of individual endosomes existed in the confocal volume at the same time. It is known that endosomes are transported from plasma membrane to the vicinity of nucleus in a few hours (21, 26, 27). Therefore, it is expected that closer to nucleus, average viscosity of endosomes become more viscous. In the future, more detailed investigation, using FCS with other methodological techniques, about time- and spatial distribution of the physiological properties of the internal space of individual endosome is required.

In summary, we first succeeded in measuring the dynamics of macromolecules ingested in endosomes and obtained interesting information about the microenvironment of endosomal internal space by using FCS. In addition we proved that FCS can be a powerful tool for the investigation of microenvironment of the internal space of organelles. This study is its first step. FCS can give information about other parameters such as relative fluorescence intensity, fluorescence yield and concentration, besides diffusional properties. Therefore it is expected that the functional and dynamic behavior of macromolecules (e.g., protein synthesis/transport and ligand–recepter interaction, etc.) in various organelles can be clarified by further investigations using FCS combined, if necessary, with other methods.

ACKNOWLEDGEMENTS

We thank Dr. T. Naiki (RIES, Hokkaido University) for the suggestion for the cell preparation, and Dr. G. Nishimura (RIES, Hokkaido University) for valuable discussions on FCS measurement.

REFERENCES

1. Thompson, N. L. (1991) Fluorescence correlation spectroscopy. *In* Topics in Fluorescence Spectroscopy: Techniques (Lakowicz, J., Ed.), Vol. 1, pp. 337–378, Plenum Press, New York.
2. Ehrenberg, M., and Rigler, R. (1974) Rotational Brownian motion and fluorescence intensity fluctuations. *Chem. Phys.* **4,** 390–401.
3. Elson, E. L., and Magde, D. (1974) Fluorescence correlation spectroscopy. I. Conceptual basis and theory. *Biopolymers* **13,** 1–27.
4. Geerts, H. (1982) A note on number fluctuations: Statistics of fluorescent correlation spectroscopy as applied to brownian motion. *Stat. Phys.* **28,** 173–176.
5. Rigler, R., Widengren, J., and Mets, Ü. (1992) Interaction and kinetics of single molecules as observed by fluorescence correlation spectroscopy. *In* Fluorescence Spectroscopy New Methods and Applications (Wolfbeis, O. S., Ed.), pp. 13–24, Springer-Verlag, Berlin.
6. Rigler, R., Mets, Ü., Widengren, W., and Kask, P. (1993) Fluorescence correlation spectroscopy with high count rate and low background: Analysis of translational diffusion. *Eur. Biophys. J.* **22,** 169–175.
7. Eigen, M., and Rigler, R. (1994) Sorting single molecules: Application to diagnostics and evolutionary biotechnology. *Proc. Natl. Acad. Sci. USA* **91,** 5740–5747.
8. Kinjo, M., and Rigler, R. (1995) Ultrasensitive hybridization analysis using fluorescence correlation spectroscopy. *Nucleic Acids Res.* **23,** 1795–1799.
9. Oehlenschläger, F., Schwille, P., and Eigen, M. (1996) Detection of HIV-1 RNA by nucleic acid sequence-based amplification combined with fluorescence correlation spectroscopy. *Proc. Natl. Acad. Sci. USA* **93,** 12811–12816.
10. Pack, C.-G., Nishimura, G., Tamura, M., Aoki, K., Taguchi, H., Yoshida, M., and Kinjo, M. (1999) Analysis of interaction between chaperonin GroEL and its substrate using fluorescence correlation spectroscopy. *Cytometry* **36,** 247–253.
11. Pack, C.-G., Aoki, K., Taguchi, H., Yoshida, M., Kinjo, M., and Tamura, M. (2000) Effect of electrostatic interactions on the binding of charged substrate to GroEL studied by highly sensitive fluorescence correlation spectroscopy. *Biochem. Biophys. Res. Commun.* **267,** 300–304, doi:10.1006/bbrc.1999.1864.
12. Berland, K. M., So, P. T. C., and Gratton, E. (1995) Two-photon fluorescence correlation spectroscopy: Method and application to the intracellular environment. *Biophys. J.* **68,** 694–701.
13. Brock, R., Vamosi, G., Vereb, G., and Jovin, T. M. (1999) Rapid characterization of green fluorescent protein fusion proteins on the molecular and cellular level by fluorescence correlation microscopy. *Proc. Natl. Acad. Sci. USA* **96,** 10123–10128.
14. Terada, S., Kinjo, M., and Hirokawa, N. (2000) Oligomeric tubulin in large transporting complex is transported via kinesin in squid giant axons. *Cell* **163,** 141–155
15. Axelrod, D., Koppel, D. E., Schlessinger, J., Elson, E., and Webb, W. W. (1976) Mobility measurement by analysis of fluorescence photobleaching recovery kinetics. *Biophys. J.* **16,** 1055–1069.

16. Luby-Phelps, K., Castle, P. E., Taylor, D. L., and Lanni, F. (1987) Hindered diffusion of inert tracer particles in the cytoplasm of mouse 3T3 cells. *Proc. Natl. Acad. Sci. USA* **84,** 4910–4913.
17. Seksek, O., Biwersi, J., and Verkman, A. S. (1987) Translational diffusion of macromolecule-sized solutes in cytoplasm and nucleus. *J. Cell Biol.* **138,** 131–142.
18. Lulacs, G. L., Haggie, P., Seksek, O., Lechardeur, D., Freedman, N., and Verkman, A. S. (2000) Size-dependent DNA mobility in cytoplasm and nucleus. *J. Biol. Chem.* **275,** 1625–1629.
19. Steinman, R. M., Mellman, I. S., Muller, W. A., and Cohn, Z. A. (1983) Endocytosis and the recycling of plasma membrane. *J. Cell Biol.* **96,** 1–27.
20. Trowbridge, I. S., Collawn, J. F., and Hopkins, C. R. (1993) Signal-dependent membrane protein trafficking in the endocytic pathway. *Annu. Rev. Cell Biol.* **9,** 129–161.
21. Mellman, I. (1996) Endocytosis and molecular sorting. *Annu. Rev. Cell Dev. Biol.* **12,** 575–625.
22. Milici, A. J., Watrous, N. E., Stukenbrok, H., and Palade, G. E. (1987) Transcytosis of albumin in capillary endothelium *J. Cell Biol.* **105,** 2603–2612.
23. Guillot, F. L., Audus, L. K., and Raub, T. J. (1990) Fluid-phase endocytosis by primary cultures of bovine brain microvessel endothelial cell monolayers. *Microvasc. Res.* **39,** 1–14.
24. Sakai, T., Mizuno, T., Miyamoto, H., and Kawasaki, K. (1998) Two distinct kinds of tubular organelles involved in the rapid recycling and slow processing of endocytosed transferrin. *Biochem. Biophys. Res. Commun.* **242,** 151–157, doi:10.1006/bbrc.1997.7577.
25. Hellevik, T., Martinez, I., Olsen, R., Toh, B.-H., Webster, P., and Smedsrød, B. (1998) Transport of residual endocytosed products into terminal lysosomes occurs slowly in rat liver endothelial cells. *Hepatology* **28,** 1378–1389.
26. Liu, S.-M., Magnusson, K.-E., and Sundqvist, T. (1993) Microtubules are involved in transport of macromolecules by vesicles in cultured bovine aortic endothelial cells. *J. Cell. Physiol.* **156,** 311–316.
27. Mellman, I., Fuchs, R., and Helenius, A. (1986) Acidification of the endocytic and exocytic pathways. *Annu. Rev. Biochem.* **55,** 663–700.
28. Benson, R. C., Meyer, R. A., Zaruba, M. E., and McKhann, G. M. (1979) Cellular autofluorescence—Is it due to flavins? *J. Histochem. Cytochem.* **27,** 44–48.
29. Ichikawa, T., Yamada, M., Homma, D., Cherry, R. J., Morrison, I. E. G., and Kawato, S. (2000) Digital fluorescence imaging of trafficking of endosomes containing low-density lipoprotein in brain astroglial cells. *Biochem. Biophys. Res. Commun.* **269,** 25–30, doi:10.1006/bbrc.2000.2261.
30. Dan, C., and Wake, K. (1985) Modes of endocytosis of latex particles in sinusoidal endothelial and Kupffer cells of normal and perfused rat liver. *Exp. Cell. Res.* **158,** 75–85.
31. Prescianotto-Baschong, C., and Riezman, H. (1998) Morphology of the yeast endocytic pathway. *Mol. Biol. Cell.* **9,** 173–189.